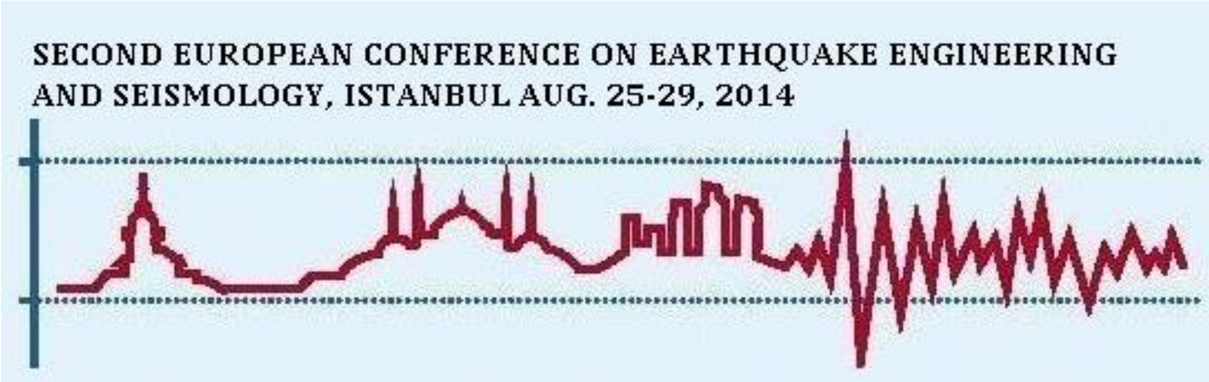

DUCTILITY AND DAMAGE EVALUATION METHOD OF STEEL COLUMNS SUBJECTED TO INELASTIC CYCLIC LOADING UNDER CONSTANT AXIAL FORCE

Shoichi Inoue[1], Takayuki Kato[2], Kenjiro Mori[3] and Takumi Ito[4]

ABSTRACT

In order to evaluate the performance of steel structures under cyclic loading of earthquake, it is necessary to simulate accurately the behavior of the structure until the ultimate states such as the buckling or the fracture of the steel members. In this paper, the database is structured, which stores the test results of the past study of H-shaped steel columns subjected to inelastic cyclic loading under constant axial force. It provides reference to strength, ductility and energy absorbing capacity until the ultimate states of the H-shaped steel columns under various experiment conditions.

The next, the prediction method considering cumulative damage is necessary to predict the capacity of H-shaped steel columns until the ultimate states under cyclic loading. Herein, they are analyzed statistically with a large number of past references from the database. The key parameters related to performance and damage evaluation are investigated and estimated by this enormous analysis. Also, the evaluation equations are established from the analysis results, which is formulated and obtained from regression analysis considering the key parameters. From the comparison of results, the proposed method for damage evaluation show good agreements with the test results of the database.

1. INTRODUCTION

In recent years, the terrible earthquake events which are unexpected in the design process have occurred in the world. From the viewpoint of the suffering due to the unexpected situations, it is desirable to ensure the structural performance such as redundancy, robustness and repairability. It can be said that the cumulative damage and residual seismic resistant performance of H-shaped steel columns after inelastic response are important indexes to establish the design guideline considering these ultimate states performance. In order to estimate these damage indexes, it is necessary to simulate accurately the behaviour of the structure until the ultimate states such as buckling or fracture of members. The ductility of H-shaped steel columns on the ultimate states show the complicated and unstable behaviour because many kinds of buckling and fractures are combined. So the experimental studies are reported all over the world by any researcher. However, the integrative studies of the knowledge are not attempted satisfactorily. Generally, it is supposed that thickness ratio, slenderness ratio and axial force are regarded as important indices on ductility of H-shaped steel columns. In this paper, the evaluation method which predicts energy absorbing capacity until maximum strength of H-shaped steel columns subjected to inelastic cyclic loading is proposed by considering the relation between these parameter and the performances such as ductility and capacity.

[1] Tokyo Univ. of Sci., 6-3-1, Niijuku, Katsushika-ku, Tokyo, Japan, dos.diosas0201@gmail.com
[2] Tokyo Univ. of Sci., 6-3-1, Niijuku, Katsushika-ku, Tokyo, Japan, yui63099@nifty.com
[3] Tokyo Univ. of Sci., 6-3-1, Niijuku, Katsushika-ku, Tokyo, Japan, j4112653@ed.tus.ac.jp
[4] Tokyo Univ. of Sci., 6-3-1, Niijuku, Katsushika-ku, Tokyo, Japan, t-ito@rs.kagu.tus.ac.jp

2. OUTLINE OF DATABASE OF PAST TEST DATA

2.1 Past Test Data of H-shaped Steel Members subjected to Cyclic Loadings

The strength, ductility and hysteresis loops of H-shaped steel columns subjected to inelastic cyclic loadings are reviewed with a large number of past references, from which a database has been structured. Total size of test data is 113 which have been reported in past papers published in Japan from 1976 to 1992. A part of the database in Japanese can be referred to the appendix.

2.2 Material Properties, Slenderness Ratio and Width - Thickness Ratio

The yield strength, Young's modulus and elongations from the material test results in the past paper have been stored in the database. However, if Young's modulus is not indicated in partly papers, these values are assumed to be taken 205GPa. Furthermore, the slenderness ratio and width-thickness ratio are calculated using the specimen in original papers, these values has been structured.

2.3 P-δ Effects

It is widely recognized that Pδ moment affects the strength and the ductility of columns. In this paper, the test results considering of Pδ moment has been stored for the database.

2.4 Loading Type and Path

The loading types are classified as; (a) cantilever-column, (b) pin-supported simple column and (c) fix-supported column, as shown in Figure1. And also, the loading paths are classified as; (a) constant amplitude cyclic loading, (b) gradual increase loading, (c) gradual decrease loading and (d) random loading.

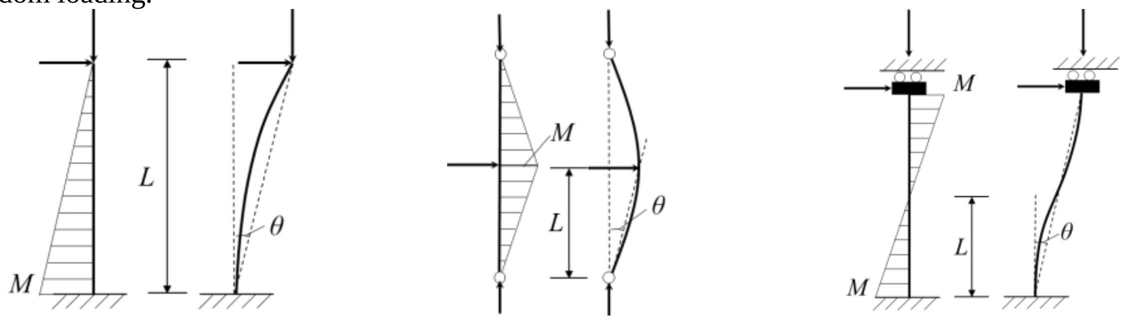

(a) cantilever-column (b) pin-supported simple column (c) fix-supported column

Figure 1. : Loading types

2.5 Failure Mode

The failure modes observed in past papers are classified as; lateral buckling and local buckling. In this paper, the phenomenon occurring in first beginning define failure mode. These failure mode shown in the papers are stored in the database. And failure modes of all test data is local buckling of flange.

2.6 Pickup Strength and Ductility on Load-Deformation Curves

From the hysteresis loops of test results, the load - cumulative deformation curve is abstracted as shown in Figure 2. And also, the strength and ductility on the curve are picked up.

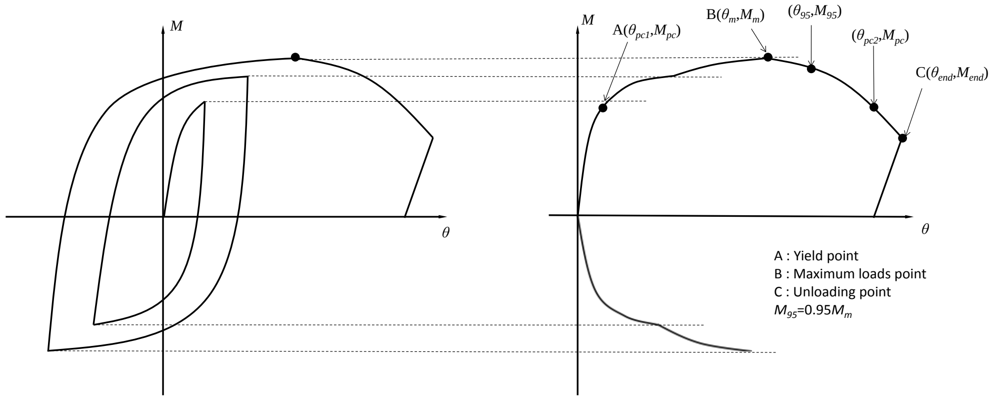

(a): hysteresis curve (b): Skeleton curve

Figure 2. : Pickup points of strength and ductility of test results

3. OBSEVATION OF STRENGTH AND DUCTILITY BY REFER OF DATABASE

3.1 Relation of Performance vs Each Parameters of Column

From the enormous analysis of database and test data of load-deformation curve, the performance of H-shaped steel columns can be estimated by the following parameters.

(1)λ_x : the general slenderness ratio of strong axis
(2)β_{eq} : the equivalent width thickness ratio
(3)N/N_y : the axial force ratio
(4)${}_s\mu_m$: the ductility of skeleton curve until the load reaches the maximum strength
(5)${}_s\eta_m$: the energy absorbing capacity on skeleton curve until the load reaches the maximum strength

Where the general slenderness ratio of strong axis λ_x is given as;

$$\lambda_x = \frac{1}{\pi}\frac{L}{i_x}\sqrt{\varepsilon_y} \qquad (1)$$

Where L is the span length as shown in Figure 1, i_x is the major axis radius of gyration, ε_y is the yield strain.

And the equivalent width thickness ratio β_{eq} is given as;

$$\beta_{eq} = \sqrt{\left(\frac{b}{t_f}\right)^2 \varepsilon_{yf} + \left(\frac{d}{t_w}\right)^2 \frac{\varepsilon_{yw}}{22}} \qquad (2)$$

Where b/t_f is flange width thickness ratio, d/t_w is web width thickness ratio, ε_{yf}, ε_{yw} are flange and web yield strain. And b, d are the width of flange and web, t_f, t_w are the thickness of flange and web, respectively as shown Figure 2.

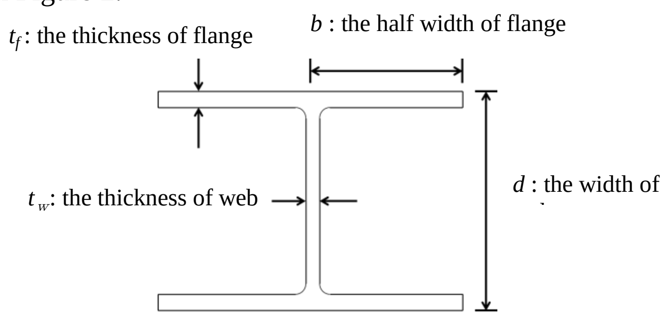

Figure 2 : Section Size

In fact, these parameters show correlations clearly between each other as shown Figures 3, 4, 5.

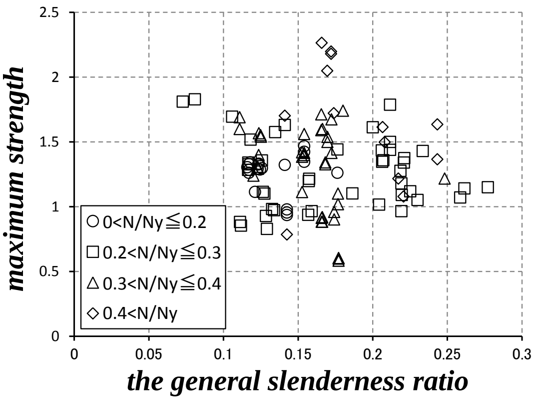

(a):maximum strength vs. the general slenderness ratio

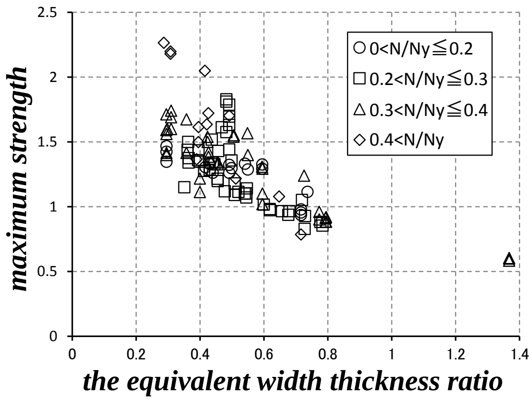

(b):maximum strength vs. the equivalent width thickness ratio

Figs.3 : maximum strength

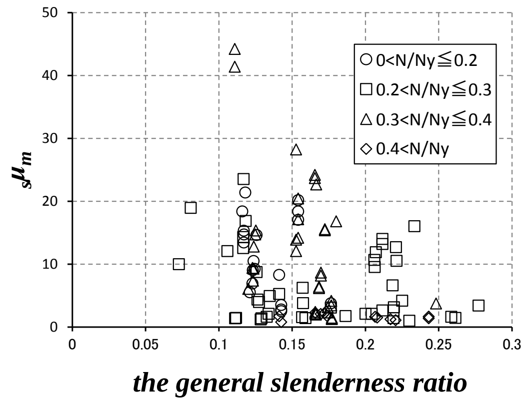

(a): $_s\mu_m$ vs. the general slenderness ratio

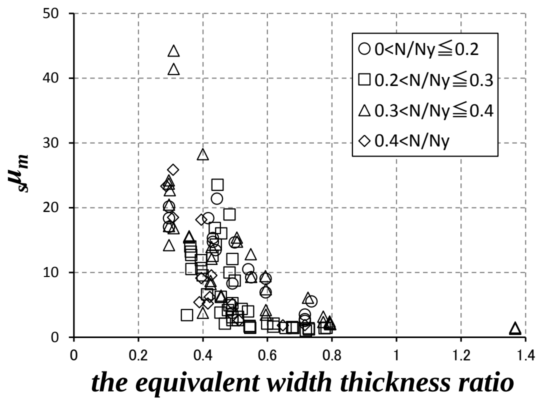

(b): $_s\mu_m$ vs. the equivalent width thickness ratio

Figs.4 : ductility of skeleton curve

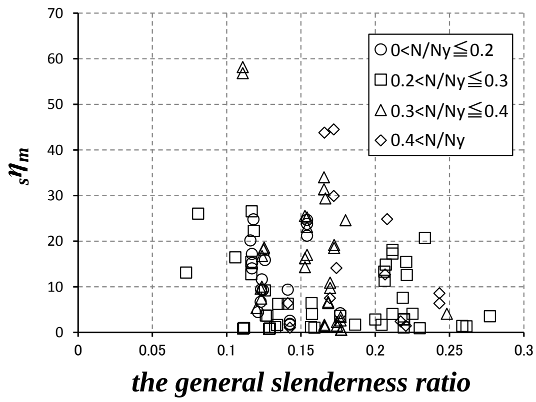

(a): $_s\eta_m$ vs. the general slenderness ratio

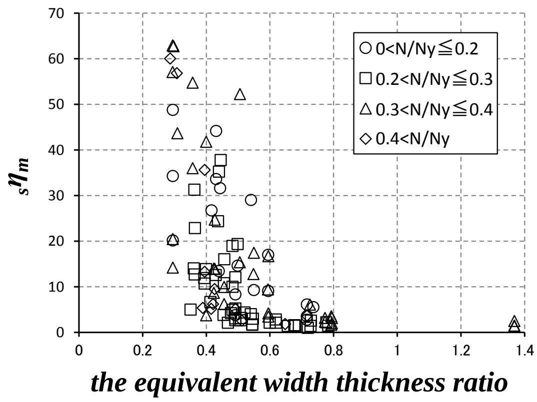

(b): $_s\eta_m$ vs. the equivalent width thickness ratio

Figs.5 : energy absorbing capacity on skeleton curve

3.2 Regression analysis

The evaluation equations are established from these results, which is formulated and obtained from regression analysis considering with key parameter

$$ {}_s\mu_m = 0.110 \times \frac{1}{\beta^2 + 0.010} \times \frac{1}{\lambda_x{}^2 + 0.020} $$
$$ \beta = (1 + 0.050 \times N / N_y)\beta_{eq} \qquad (3) $$

Also, from the Figure 6, the relation between ${}_s\mu_m$ and ${}_s\eta_m$ is formulized as;

$$ {}_s\eta_m = 0.73 \times {}_s\mu_m{}^{1.21} \qquad (4) $$

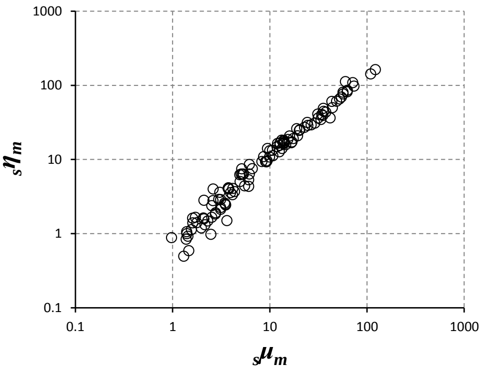

Figs.6 : ${}_s\eta_m$ vs. ${}_s\mu_m$

Figure 7 shows comparison of regression analysis and test results categorized N/N_y. As shown in this figure, the evaluation method has good agreements with the test results in the database.

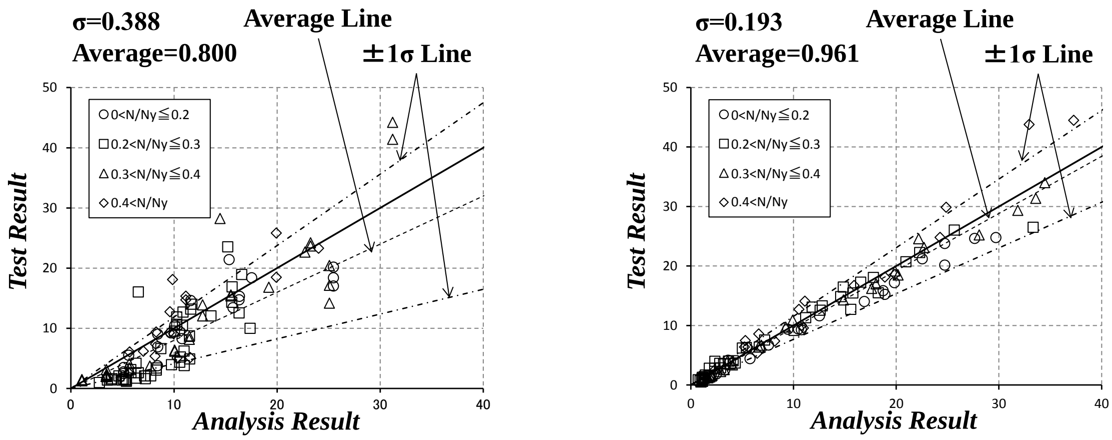

(a)Equations 3. And Test Results (b) Equations 4. And Test Results

Figs.7 : Comparison of Proposed Method and Test Results

4. PROPOSAL OF PREDICTION METHODS FOR ENERGY CAPACITY

4.1 Evaluation of Energy Absorbing Capacity

According to the database and Figure 8, high correlation between energy absorbing capacity and cyclic indexes such as cycle number and loading path is confirmed. This relation derives that the equation which predicts cumulative plastic capacity is formulized as;

$$\frac{{}_c\eta_m}{{}_s\eta_m} = 2c(1-\gamma_m)N_{em}{}^k + 2\gamma_m - 1 \tag{5}$$

where ${}_c\eta_m$ is the cumulative plastic capacity, and c, k are constants. Furthermore, the constants are determined from the database, and it is given as c = 1.72, k = 0.30. N_{em} is the effective half cycle number and γ_m is the amplitude deviation defined in next section.

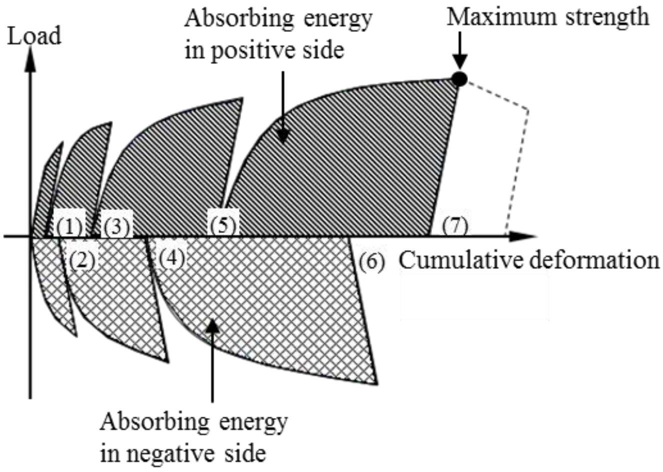

Figure8 : Relation between absorbing energy and cycle umber

4.1.1 Cycle Number until Maximum Strength : N_{em}

In this paper, a half cycle is defined as one cycle illustrated as Figure 9. As shown in this figure, a half cycle over 5% energy of maximum absorbing energy is regarded as effective cycle. It means that the cycle less than 5% is ignored. And also, N_{em} is defined as the sum of the effective cycle. According to this model, a cycle with small amplitude after the large amplitude experienced is not ignored. In this example as shown in Figure 9, the cycle number until maximum strength is counted as 7, but the effective cycle number is counted as 5. The above cycle is renewed at each cycle by consideration with the effective cycle which would cause the plastic damage.

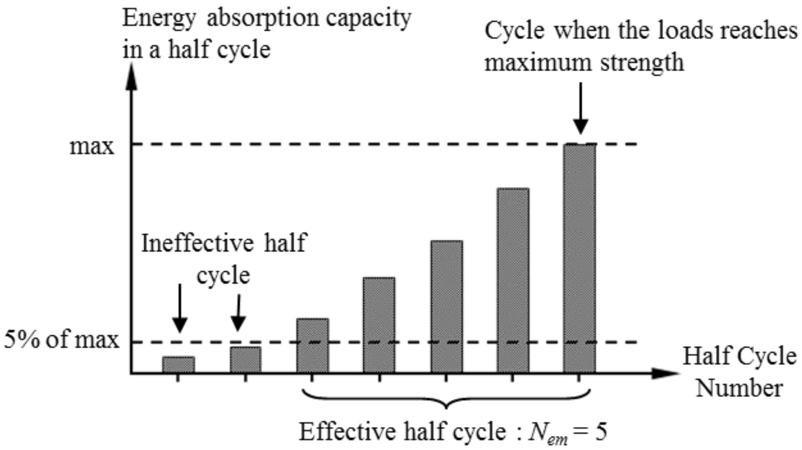

Figure9 : Example of half cyclic absorbing energy and effective cyclic number

4.1.2 Deviation of Amplitude until Maximum Strength : γ_m

An index γ_m which means the deviation of the amplitude until a load reaches the maximum strength is defined as;

$$\gamma_m = \frac{\max\{{}_c\eta_{m(+)}, {}_c\eta_{m(-)}\}}{{}_c\eta_m} \tag{6}$$

where ${}_c\eta_m$ (+) is the absorbed energy on the positive side, ${}_c\eta_m$ (-) is the absorbed energy on the negative side as shown in Figure 2.1-(c). If the same amplitude in positive and negative side is loaded, γ_m becomes 0.5. And the unidirectional such as monotonic loading is loaded, γ_m becomes 1.0.

4.2 Comparison of Proposed Method and Test Results

Figure 10 shows comparison of proposed method and test results categorized γ_m. As shown in this figure, the evaluation method has good agreements with the test results in the database.

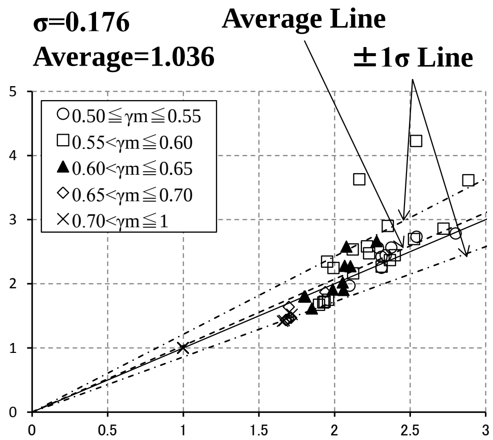

Figure10 : Comparison of Proposed Method and Test Results

5. CONCLUSIONS

In this paper, the database which stores the test results of the enormous past study on steel column subjected to inelastic cyclic loading under constant axial force is structured.
Also, the evaluation method, which predicts the ductility and energy absorbing capacity at the maximum strength of the steel column subjected to cyclic loadings under constant axial force, was formulated by the references in the database of a large number of past references. This method has good agreements with the test results in the database.

REFERENCES

Kenjiro Mori and Takumi Ito (2012). *Proposal of hysteresis Model and Damage Evaluation Method of Steel Beams Subjected to Inelastic Cyclic Loading*, Vol.15 : Issue WCEE

Takayuki Kato, Kenjiro Mori and Takumi Ito (2013).*Ductility and Damage Evaluation Method of Steel Columns Subjected to Inelastic Cyclic Loading Under Constant Axial Force*, The Pacific Structural Steel Conference

Appendix

*1) Meaning of each alphabet are shown in the chapter 2.
*2) Grade of JIS (Japan Industrial Standards)
*3) M_{pc} is full plastic moment considering axial force.

Table1. A part of the Database

ID	Section Size				Span length	Material Property of flange		N/Ny	Loading Type*1	Loading Path*1	Test Results					
	H	B	t_w	t_f	L	σ_y	E				M_m/M_{pc} *3	${}_s\mu_m$	${}_s\eta_m$	${}_c\eta_m$	γ_m	N_{em}
[-]	[mm]	[mm]	[mm]	[mm]	[mm]	[Mpa]	[Gpa]	[-]	[-]	[-]	[-]	[-]	[-]	[-]	[-]	[-]
1	125	125	6.5	9	750	280	206	0.33	(c)	(a)	1.599	22.65	29.34	81.69	0.536	6
2	125	125	6.5	9	700	276	206	0.17	(b)	(a)	1.346	20.16	24.63	24.63	1	1
3	125	125	6.5	9	700	276	206	0.17	(b)	(a)	1.466	18.38	23.77	60.90	0.537	3
4	125	125	6.5	9	700	276	206	0.33	(b)	(a)	1.415	20.42	25.20	25.20	1	1
5	125	125	6.5	9	700	276	206	0.33	(b)	(a)	1.397	14.16	16.98	16.98	1	1
6	125	125	6.5	9	700	276	206	0.33	(b)	(a)	1.560	17.14	23.11	97.64	0.569	5
7	125	125	6.5	9	700	276	206	0.17	(b)	(a)	1.423	17.03	21.20	40.33	0.619	3
8	125	125	6.5	9	780	551	205	0.5	(b)	(a)	1.365	5.36	6.36	6.36	1	1
9	125	125	6.5	9	780	256	205	0.5	(b)	(a)	2.265	23.30	43.77	112.23	0.505	3
10	125	125	6.5	9	780	551	205	0.5	(b)	(a)	1.634	6.18	8.57	8.57	1	1
11	125	125	6.5	9	780	574	205	0.33	(b)	(a)	1.217	3.73	4.07	4.07	1	1
12	125	125	6.5	9	780	302	205	0.33	(b)	(a)	1.740	16.81	24.56	60.76	0.558	3
13	125	125	6.5	9	480	574	205	0.33	(b)	(a)	1.112	28.24	25.51	36.40	0.701	2
14	125	125	6.5	9	480	302	205	0.33	(b)	(a)	1.599	44.21	58.17	142.14	0.519	3
15	125	125	6.5	9	480	302	205	0.33	(b)	(a)	1.690	41.40	56.83	162.49	0.557	6
16	125	125	6.5	9	480	574	205	0.33	(b)	(a)	1.385	13.89	16.22	16.22	1	1
17	125	125	6.5	9	480	574	205	0.33	(b)	(a)	1.419	12.07	14.27	28.82	0.620	3
18	125	125	6.5	6	750	297	205	0.67	(c)	(a)	1.722	9.49	14.07	14.07	1	1
19	125	125	6.5	6	750	282	205	0.67	(c)	(a)	2.049	5.15	7.47	7.47	1	1
20	125	125	3.2	3.2	750	287	206	0.33	(c)	(a)	0.913	2.15	1.35	2.43	0.639	2
21	125	125	3.2	3.2	750	287	206	0.33	(c)	(a)	0.882	2.37	1.61	1.61	1	1
22	125	125	6	6	750	288	206	0.33	(c)	(a)	1.537	8.64	10.89	10.89	1	1
23	125	125	6	6	750	288	206	0.33	(c)	(a)	1.499	8.15	9.72	17.52	0.642	2
24	125	125	3.2	3.2	750	287	205	0.33	(c)	(a)	0.918	2.00	1.24	2.13	0.581	2
25	125	125	3.2	3.2	750	287	205	0.33	(c)	(a)	0.883	1.97	1.19	1.19	1	1
26	125	125	2	2	750	332	205	0.33	(c)	(a)	0.603	1.27	0.52	0.98	0.662	3
27	125	125	2	2	750	332	205	0.33	(c)	(a)	0.582	1.30	0.50	0.50	1	1
28	125	125	2	2	750	332	205	0.33	(c)	(a)	0.599	1.47	0.59	0.59	1	1
29	125	125	3.05	3.05	750	212	205	0.17	(c)	(a)	0.955	3.49	2.50	2.50	1	1
30	125	125	3.05	3.05	750	212	205	0.17	(c)	(a)	0.935	2.76	1.84	1.84	1	1
31	125	125	3.05	3.05	750	212	205	0.17	(c)	(a)	0.978	2.50	1.68	4.34	0.563	3
32	125	125	3.05	3.05	750	212	205	0.67	(c)	(a)	0.785	1.82	0.98	1.50	0.741	3
33	125	125	4.5	6	750	297	205	0.33	(c)	(a)	1.327	6.17	6.37	6.37	1	1
34	125	125	4.5	4.5	750	319	205	0.33	(c)	(a)	1.019	3.44	2.58	2.58	1	1
35	125	125	4.5	3.2	750	294	205	0.33	(c)	(a)	0.900	2.31	1.48	1.48	1	1
36	125	125	4.5	9	750	315	205	0.33	(c)	(a)	1.414	15.54	18.46	44.67	0.528	3
37	125	125	4.5	9	750	315	205	0.33	(c)	(a)	1.673	15.35	19.13	69.36	0.581	3
38	125	125	4.5	6	750	297	205	0.33	(c)	(a)	1.341	6.37	6.67	10.77	0.619	2
39	125	125	4.5	4.5	750	319	205	0.33	(c)	(a)	1.100	4.13	3.35	3.35	1	1
40	125	125	4.5	3.2	750	294	205	0.33	(c)	(a)	0.959	3.13	2.24	2.24	1	1
41	125	125	6	9.5	750	279	205	0.33	(c)	(a)	1.590	23.68	31.36	85.70	0.520	4
42	125	125	6	9.5	750	279	205	0.33	(c)	(a)	1.712	24.19	34.00	76.48	0.529	3
43	125	125	6	9.5	750	302	205	0.67	(c)	(a)	2.198	18.46	29.87	80.55	0.573	5
44	125	125	6	9.5	750	302	205	0.67	(c)	(a)	2.179	25.81	44.47	108.75	0.565	4
45	130.8	120.6	6	5.7	500	360	193	0.3	(b)	(b)	1.357	8.74	9.16	20.88	0.616	3
46	130.8	120.6	6	5.7	500	360	193	0.2	(b)	(d)	1.296	14.61	15.84	15.84	1	1
47	132	120.3	6	5.6	500	360	193	0.4	(b)	(b)	1.551	14.72	18.13	65.48	0.573	8
48	131.7	120.2	6	5.6	500	360	193	0.4	(b)	(d)	1.539	15.35	18.57	18.57	1	1
49	131.1	180.6	6	5.5	500	360	193	0.2	(b)	(d)	1.114	5.52	4.41	4.41	1	1
50	132.1	180.8	6	5.6	500	360	193	0.4	(b)	(d)	1.239	6.06	5.31	5.31	1	1

ID	Section Size				Span length	Material Property of flange		N/Ny	Loading Type[*1]	Loading Path[*1]	Test Results					
	H	B	t_w	t_f	L	σ_y	E				M_m/M_{pc}[*3]	$_s\mu_m$	$_s\eta_m$	$_c\eta_m$	γ_m	N_{em}
[-]	[mm]	[mm]	[mm]	[mm]	[mm]	[Mpa]	[Gpa]	[-]	[-]	[-]	[-]	[-]	[-]	[-]	[-]	[-]
51	131.8	132.5	6	5.7	500	360	193	0.2	(b)	(b)	1.332	10.48	11.61	30.92	0.642	5
52	132	132.7	6	5.6	500	360	193	0.4	(b)	(b)	1.399	9.26	10.01	19.10	0.645	3
53	131.6	145.2	6	5.6	500	360	193	0.2	(b)	(b)	1.292	6.91	6.69	17.26	0.612	3
54	131.2	145.4	6	5.6	500	360	193	0.4	(b)	(b)	1.292	7.36	7.38	16.77	0.602	3
55	131.1	132.8	6	5.6	500	360	193	0.2	(b)	(d)	1.287	9.25	9.28	9.28	1	1
56	131.9	132.3	6	5.6	500	360	193	0.4	(b)	(d)	1.566	12.76	16.72	16.72	1	1
57	131.3	145.2	6	5.6	500	360	193	0.2	(b)	(d)	1.325	9.04	9.39	9.39	1	1
58	131.6	145	6	5.6	500	360	193	0.4	(b)	(d)	1.308	9.39	9.57	9.57	1	1
59	120.4	119.8	5.8	5.6	500	275	199	0.2	(b)	(a)	1.283	14.72	15.23	34.53	0.591	4
60	120.8	120	5.9	5.6	500	275	199	0.2	(b)	(a)	1.328	15.32	17.19	49.85	0.579	4
61	121.7	119.4	5.9	5.8	500	275	199	0.2	(b)	(a)	1.305	18.38	20.15	29.27	0.688	2
62	119.8	119.6	5.8	5.4	500	275	199	0.2	(b)	(a)	1.342	21.40	24.77	36.37	0.681	2
63	120.2	119.7	5.6	5.5	500	275	199	0.2	(b)	(a)	1.262	13.42	14.01	14.01	1	1
64	120.9	120.1	5.7	5.5	500	275	199	0.3	(b)	(a)	1.340	14.31	15.47	39.23	0.597	3
65	119.2	119.4	5.7	5.5	500	275	199	0.3	(b)	(a)	1.517	16.87	22.23	31.53	0.705	2
66	121.1	119.3	5.8	5.6	500	275	199	0.3	(b)	(a)	1.283	12.54	12.71	12.71	1	1
67	120.7	119.6	5.7	5.4	500	275	199	0.3	(b)	(a)	1.326	23.52	26.50	43.43	0.687	2
68	150	75	3.2	4.5	536	303	205	0.3	(c)	(c)	1.695	12.06	16.45	16.45	1	1
69	150	75	3.2	4.5	714	303	205	0.15	(c)	(c)	1.322	8.29	9.36	9.36	1	1
70	150	75	3.2	4.5	714	303	205	0.3	(c)	(c)	1.630	5.23	6.27	6.27	1	1
71	150	75	3.2	4.5	714	303	205	0.6	(c)	(c)	1.701	5.09	6.37	6.37	1	1
72	150	75	3.2	4.5	1071	303	205	0.3	(c)	(a)	1.787	2.61	3.99	3.99	1	1
73	150	75	3.2	4.5	375	292	205	0.3	(c)	(a)	1.811	9.98	13.07	13.07	1	1
74	150	75	3.2	4.5	417	292	205	0.3	(c)	(a)	1.828	18.95	26.02	26.02	1	1
75	150	75	3.2	4.5	893	303	205	0.15	(c)	(a)	1.261	3.77	4.16	4.16	1	1
76	150	75	3.2	4.5	893	303	205	0.3	(c)	(c)	1.441	3.06	3.61	3.61	1	1
77	150	75	3.2	4.5	694	292	205	0.3	(c)	(c)	1.575	4.92	6.21	6.21	1	1
78	150	75	3.2	4.5	1071	271	205	0.3	(c)	(c)	1.612	2.10	2.81	2.81	1	1
79	100.1	100.4	5.82	5.78	750	306	205	0.3	(a)	(c)	1.341	12.69	15.45	15.45	1	1
80	95	100.8	6.17	4.38	750	297	205	0.3	(a)	(c)	1.430	16.02	20.69	20.69	1	1
81	100.1	99.6	4.51	6.12	750	294	205	0.3	(a)	(c)	1.438	13.99	18.06	18.06	1	1
82	99.9	99.2	4.47	4.5	750	325	205	0.3	(a)	(c)	1.119	4.18	4.07	4.07	1	1
83	100.4	99.9	3.27	6.3	750	294	205	0.3	(a)	(c)	1.434	10.66	13.29	13.29	1	1
84	99.6	99.5	3.24	4.51	750	325	205	0.3	(a)	(c)	1.091	3.13	2.87	2.87	1	1
85	100	99.8	3.26	3.24	750	316	205	0.3	(a)	(c)	0.965	1.40	1.06	1.06	1	1
86	135.3	100.3	3.13	6.62	750	312	205	0.3	(a)	(c)	1.215	3.79	3.99	3.99	1	1
87	134.6	99.7	3.17	3.17	750	288	205	0.3	(a)	(c)	0.965	1.41	1.00	1.00	1	1
88	168.9	102.2	3.13	6.14	750	312	205	0.3	(a)	(c)	1.101	3.95	3.57	3.57	1	1
89	169.4	99.4	3.12	4.53	750	331	205	0.3	(a)	(c)	0.972	2.10	1.58	1.58	1	1
90	169.5	99.7	3.16	3.18	750	288	205	0.3	(a)	(c)	0.829	1.38	0.84	0.84	1	1
91	199.2	99.5	3.12	3.14	750	288	205	0.3	(a)	(c)	0.853	1.44	0.92	0.92	1	1
92	100.7	100.3	3.27	4.51	750	325	205	0.6	(a)	(c)	1.217	2.54	2.39	2.39	1	1
93	99.4	99	3.27	3.26	750	316	205	0.6	(a)	(c)	1.078	1.78	1.41	1.41	1	1
94	137.8	135.3	6.38	6.38	1000	456	205	0.3	(a)	(c)	1.071	1.62	1.40	1.40	1	1
95	98.7	101	3.29	5.85	750	320	205	0.3	(a)	(c)	1.277	6.62	7.53	7.53	1	1
96	99.7	100.9	3.25	5.85	750	293	205	0.3	(a)	(c)	1.358	11.88	14.84	14.84	1	1
97	99.1	100.2	3.2	3.32	750	271	205	0.3	(a)	(c)	1.016	2.08	1.62	1.62	1	1
98	101	99.5	3.22	3.39	750	234	205	0.3	(a)	(c)	1.101	1.72	1.66	1.66	1	1
99	100	100.5	5.85	5.77	750	306	205	0.3	(a)	(a)	1.374	10.53	12.56	27.16	0.596	3
100	101	99.7	4.46	6.08	750	300	205	0.3	(a)	(a)	1.500	13.18	17.27	40.93	0.574	4
101	100.3	99.9	3.27	6.18	750	294	205	0.3	(a)	(a)	1.345	9.54	11.30	16.61	0.680	2
102	135.6	100.2	3.13	6.61	750	312	205	0.3	(a)	(a)	1.198	6.22	6.38	11.18	0.571	2
103	170.2	98.2	3.13	6.69	750	312	205	0.3	(a)	(a)	1.114	4.35	3.69	3.69	1	1
104	99.8	99.7	3.27	4.51	750	325	205	0.3	(a)	(a)	1.180	2.61	2.79	2.79	1	1
105	169.4	99.4	3.12	4.49	750	325	205	0.3	(a)	(a)	0.982	1.62	1.11	1.90	0.585	2
106	99.4	99.7	3.08	3.09	750	345	205	0.3	(a)	(a)	1.051	0.98	0.88	0.88	1	1
107	136.6	99.4	3.17	3.2	750	288	205	0.3	(a)	(a)	0.937	1.56	1.13	1.13	1	1
108	170.4	99.4	3.16	3.17	750	288	205	0.3	(a)	(a)	0.927	1.19	0.71	1.66	0.574	2
109	200.2	99.6	3.13	3.19	750	288	205	0.3	(a)	(a)	0.881	1.38	0.79	1.32	0.598	2
110	137.2	75.7	6.43	6.43	1000	456	205	0.3	(a)	(a)	1.149	3.38	3.50	5.04	0.695	2
111	136.2	135.6	6.36	6.36	1000	456	205	0.3	(a)	(a)	1.141	1.42	1.29	2.90	0.555	2
112	99.5	100.2	3.28	6.27	750	294	205	0.6	(a)	(c)	1.498	18.10	24.80	48.85	0.508	2
113	100.2	100.1	3.29	6.28	750	294	205	0.6	(a)	(a)	1.614	9.08	12.69	18.22	0.696	2